academicJournals

Vol. 8(8), pp. 302-309, 28 February, 2013
DOI: 10.5897/IJPS2013.3855
ISSN 1992-1950 © 2013 Academic Journals
http://www.academicjournals.org/IJPS

International Journal of Physical Sciences

Full Length Research Paper

Effects of growth rate on the physical and mechanical properties of Sn-3.7Ag-0.9Zn eutectic alloy

U. Böyük[1]*, S. Engin[2], H. Kaya[1], N. Maraşli[3], E. Çadirli[4] and M. Şahin[4]

[1]Department of Science Education, Education Faculty, Erciyes University, Kayseri, Turkey.
[2]Department of Physics, Institute of Science and Technology, Erciyes University, Kayseri, Turkey.
[3]Department of Physics, Faculty of Science, Erciyes University, Kayseri, Turkey.
[4]Department of Electronics and Automation, Technical Vocational School of Sciences, Niğde University, Niğde, Turkey.

Accepted 27 February, 2013

Sn-3.7wt.%Ag-0.9wt.%Zn alloy was directionally solidified upward under different conditions, with different growth rates (V = 3.38 - 220.12 µm/s) at a constant temperature gradient (G = 4.33 K/mm) and with different temperature gradients (G = 4.33 -12.41 K/mm) at a constant growth rate (V = 11.52 µm/s) by using a Bridgman-type directional solidification furnace. The microstructure was observed to be a rod Ag_3Sn structure in the matrix of β-Sn from the directionally solidified Sn-3.7wt.%Ag-0.9wt.%Zn samples. The microhardness, tensile strength and electrical resistivity of alloy were measured from directionally solidified samples. The dependency of the microhardness, tensile strength and electrical resistivity on the solidification parameters for directionally solidified Sn-Ag-Zn eutectic alloy was investigated and the relationships between them were experimentally obtained by using regression analysis. The results obtained in the present work were compared with the previous similar experimental results.

Key words: Alloys, crystal growth, microstructure; mechanical properties, electrical properties.

INTRODUCTION

Solidification and melting are transformations between the crystallographic and non-crystallographic states of a metal or alloy. These transformations are basic to such technological applications as ingot and continuous casting, and directionally solidification of composites and single crystals. An understanding of the mechanism of solidification and how it is affected by such parameters as temperature distribution, solidification condition and alloying, are important in the control of the mechanical and electrical properties of cast metals and fusion welds (Porter and Easterling, 1992). Most Sn-based lead-free solders contain only minor amounts of alloying additions. For example, in the widely studied Sn–Ag–Cu (SAC) alloy, more than 95% of the solder is Sn, as measured by weight (Anderson et al., 2001).

However, in these solders, the thick Cu6Sn5 IMC (intermetallic compound) layer and large Ag3Sn primary phase are often reported to influence the integrity and reliability of solder joints (Kang and Sarkhel, 1994; Jeong et al., 2004; Jo et al., 2008; Kang et al., 2003). Reducing Ag and Cu content, as well as adding minor alloying elements such as Zn, In, Bi, Co, Ni in Sn-based solder, was recently proposed in order to improve the reliability of the Pb-free solder joint (Choi et al., 2001; Seo et al., 2006, 2007; Kim et al., 2009; Cho et al., 2007; Kang et al., 2008). Although, Sn–Ag solder has great properties of

*Corresponding author. E-mail: boyuk@erciyes.edu.tr. Tel: +90 352 207 66 66 # 37096. Fax: +90 352 437 88 34.

strength, resistance to creep and thermal fatigue (Abtew and Selvaduray, 2000; Wu et al., 2004; Zeng and Tu, 2002) the small addition of Zn can improve the mechanical performance at no cost to ductility and wettability. In addition, the combination of Zn and Ag dramatically reduces corrosion potential (Knott et al., 2005).

Previous works for the Sn–Ag–Zn lead-free solder had been done mainly focused on the formation of the interfacial structure, the phase equilibria and the mechanical properties (Xu et al., 2010; Wang et al., 2009; Wei et al., 2009; Liu et al., 2008). For a system with such promising applications, however, studies considering the directional solidification of Sn-Ag-Zn alloys are rather scarce. Until now, few numbers of researches have been carried out on the characterization, physical and mechanical properties. The aim of the present work was to investigate the mechanical, electrical and thermal properties Sn-3.7wt.%Ag-0.9wt.%Zn alloy. For this purpose, the dependency of microhardness (HV), tensile strength (σ_t) and electrical resistivity (ρ) on the solidification processing parameters (G and V) for directionally solidified Sn-3.7wt.%Ag-0.9wt.%Zn alloy was investigated.

EXPERIMENTAL PROCEDURE

In the present work, the experimental procedure consists of alloy preparation, the measurements of the microhardness, tensile strength and electrical resistivity of the directionally solidified Sn-3.7wt.%Ag-0.9wt.%Zn alloy.

Alloy preparation

Using a vacuum melting furnace and a hot filling furnace, Sn-3.7wt.%Ag-0.9wt.%Zn eutectic alloy was prepared under vacuum atmosphere by melting tin, silver and zinc of high purity (>99.9 %). After allowing time for the melt homogenization, the molten alloy was poured into 13 cylindrical graphite crucibles (200 mm in length, 4 mm inner diameter and 6.35 mm outer diameter) held in a specially constructed casting furnace (hot filling furnace) at approximately 50 K above the melting point of the alloy. The molten alloy was directionally solidified from bottom to top to ensure that the crucible was completely full.

Solidification of Sn-Ag-Zn eutectic alloy was carried out with different growth rates (V = 3.38 - 220.12 μm/s) at a constant temperature gradient (G = 4.33 K/mm) and with different temperature gradients (G = 4.33 - 12.41 K/mm) at a constant growth rate (V = 11.52 μm/s) in the Bridgman–type growth apparatus. The temperature of water in the reservoir was kept at 283 K to an accuracy of ± 0.01 K using a *Poly Science digital 9102* model heating / refrigerating circulating bath to get a well quenched solid–liquid interface. The temperature of the sample was also controlled to an accuracy of ± 0.1 K degrees with a *Eurotherm 2604* type controller. The details of the apparatus and experimental procedures are given in Refs (Gündüz et al., 2004; Böyük et al., 2009). The quenched samples were removed from the graphite crucible and cut into lengths of typically 3 mm. After the metallographic process, the microstructures of the samples were revealed. Typical images of growth morphologies of directionally solidified Sn-Ag-Zn eutectic alloy are shown in Figure 1. While the cooling rate is so slow (about 0.16 K/s) that it could be considered as an equilibrium solidification process, which corresponds to an eutectic reaction: L→ AgZn +Ag_3Sn + Sn (Wei et al., 2008). It follows that β-Sn, AgZn and Ag_3Sn phases will separate out in the slowly cooled solder and eutectic microstructure consist of a mixture of ζ-AgZn and Ag_3Sn intermetallic compounds in a matrix of β-Sn (Wei et al., 2008). But, in this work were observed only rod Ag_3Sn IMC in a matrix of β-Sn as shown in Figure 1, because the cooling rate range is fairly above 0.16 K/s.

The measurement of microhardness

One of the purposes of this investigation was to learn the relationships between the solidification processing parameters and microhardness for the directionally solidified Sn–Ag–Zn eutectic alloy. The mechanical properties of solidified materials are generally determined by a hardness test, tensile strength test, etc. The Vickers hardness (HV) is the ratio of a load applied to the indenter to the surface area of the indentation. This is given by:

$$HV = \frac{2P \sin(\theta/2)}{d^2} \quad (1)$$

where HV is the Vickers microhardness in kg/mm^2, P is the applied load (kg), d is the mean diagonal of the indentation (mm) and θ is the angle between opposite faces of the diagonal indenter (136°). Microhardness measurements in this study were made with a *Future–Tech FM–700* model hardness measuring test device using 500 g load and a dwell time of 10 s giving a typical indentation depth of about 40–60 μm. The average microhardness is achieved by measuring at least 30 different points on the transverse sections. Variations of microhardness with growth rates and temperature gradients for the Sn-3.7wt.%Ag-0.9wt.%Zn eutectic alloy is plotted in Figures 2 and 3, respectively, and compared with the previous experimental results for Sn-3.5wt.%Ag-0.9wt.%Cu (Böyük and Maraşli, 2009; Çadirli and Şahin, 2012) and Sn-3.5wt.%Ag (Çadirli and Şahin, 2012; Böyük and Maraşli, 2010) eutectic alloys.

Measurement of tensile strength

The uniaxial tensile test was performed at room temperature at a strain rate of 10^{-3} s^{-1} with a *Shimadzu Universal Testing Instrument* (Type AG–10KNG) which was designed for testing the stress–strain responses of solders. In order to avoid damaging the sample surface, two seals were stuck to the sample instead of the traditional clip gauge. Strains were then measured by observing the displacement between the two seals using a video camera. A computer with a data acquisition software was used to collect the data. The data collected from the tensile test can be analyzed to determine the strength (σ) using the following formula,

$$\sigma = \frac{F}{A} \quad (2)$$

where σ is the strength in N/mm^2 (or MPa), F is the applied force (N) and A is the original cross sectional area (mm^2) of the sample. The round rod tensile samples with a diameter of 4 mm and a gauge length of 20 mm were prepared from directionally solidified rod samples with different solidification parameters. The tensile axis was chosen parallel to the growth direction of the sample and the tests were repeated three times. Variations of tensile strength with growth rate and temperature gradient for the Sn-3.7wt.%Ag-0.9wt.%Zn eutectic alloy is plotted in Figures 4 and 5, respectively, and compared with binary Sn-3.5wt.%Ag (Çadirli and Şahin, 2012)

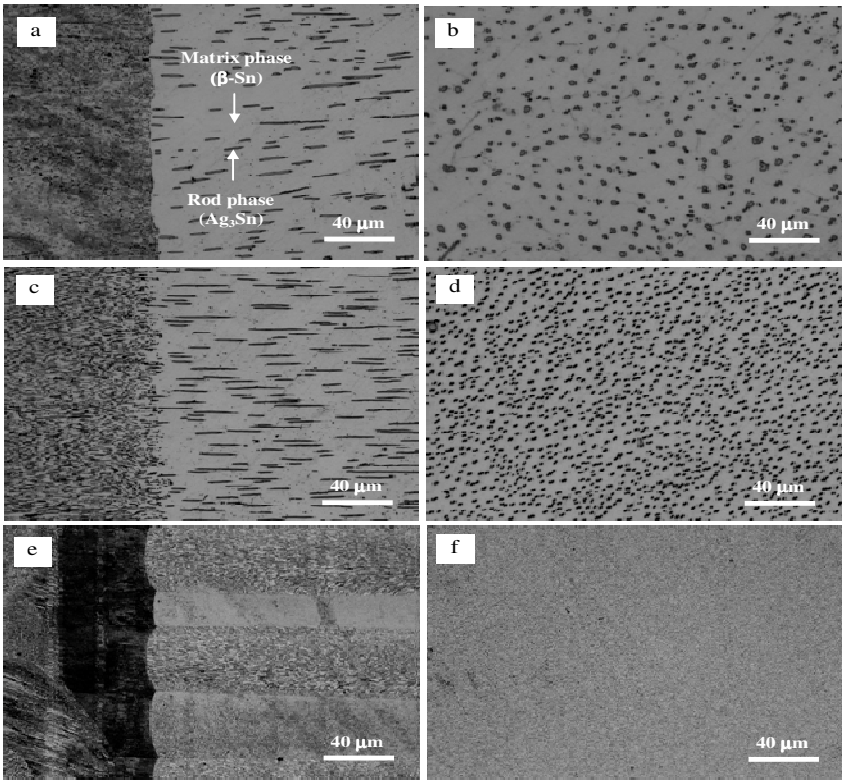

Figure 1. Typical optical images of the growth morphologies of directionally solidified Sn-3.7wt.%Ag-0.9wt.%Zn eutectic alloy, (a) longitudinal section (b) transverse section (V=3.38 µm/s, G=4.33 K/mm), (c) longitudinal section (d) transverse section, (V=11.52 µm/s, G=12.41 K/mm) (e) longitudinal section (f) transverse section (V=220.12 µm/s, G=4.33 K/mm).

eutectic alloys. It can be seen from Figures 4 and 5, the values of tensile strength for the Sn-3.7wt.%Ag-0.9wt.%Zn eutectic alloy increase with increasing the values of V and G.

The measurement of electrical resistivity

Electrical resistivity is an imperative physical property. Impurities observed in metals distort the metal lattice and can affect the behavior of ρ to a considerable extent. This is particularly true for metal alloys. The value of the electrical resistivity is also affected by grain size (e.g., higher ρ corresponds to finer grain), plastic deformation, heat treatment, and some other factors, but to a smaller extent compared to the effect of temperature and chemical composition (Rudnev et al., 2003).

The growth rate, temperature gradient and temperature dependence of electrical resistivity for Sn-3.7wt.%Ag-0.9wt.%Zn alloys were measured by the four-point probe method. A *Keithley 2400* source meter was used to provide constant current, and the potential drop was measured by a *Keithley 2700* multimeter through an interface card, which was controlled by a computer. Platinum wires with a diameter of 0.5 mm were used as current and potential probes. The voltage drop was detected, and the electrical resistivity and conductivity were determined using a standard conversion method.

The electrical resistivities of the directionally solidified Sn-3.7wt.%Ag-0.9wt.%Zn eutectic alloys were measured by the d.c. four-point probe method at room temperature. Variations of electrical resistivity with growth rate, temperature gradient and temperature for the Sn-3.7wt.%Ag-0.9wt.%Zn eutectic alloy is plotted in Figures 6 and 7, respectively. It can be seen from Figures 6 to 7, the values of electrical resistivity for the Sn–Ag–Zn eutectic alloy increase with increasing the values of V and G.

RESULTS AND DISCUSSION

The effect of solidification parameters on microhardness

It can be also seen from Figures 2 and 3 that an increase in solidification parameters leads to an increase in the HV. The dependence of the HV on V and G were determined by linear regression analysis and the relationship between them can be expressed as;

$$HV = k_1 (V)^a \quad (3)$$

$$HV = k_2 (G)^b \quad (4)$$

where k is a constant, a and b are the exponent values relating to the growth rate and temperature gradient respectively.

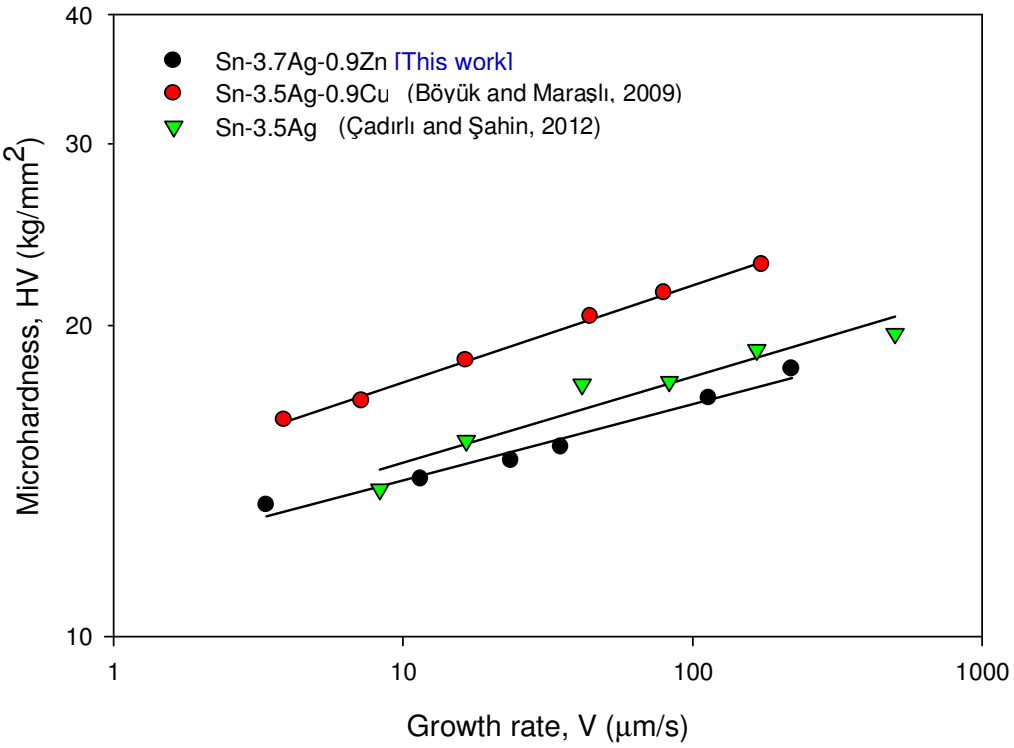

Figure 2. Variation of microhardness, as a function of growth rate for directionally solidified Sn-3.7wt.%Ag-0.9wt.%Zn eutectic alloy at a constant temperature gradient and compare with the Sn-3.5wt.%Ag-0.9wt.%Cu and Sn-3.5wt.%Ag eutectic alloys.

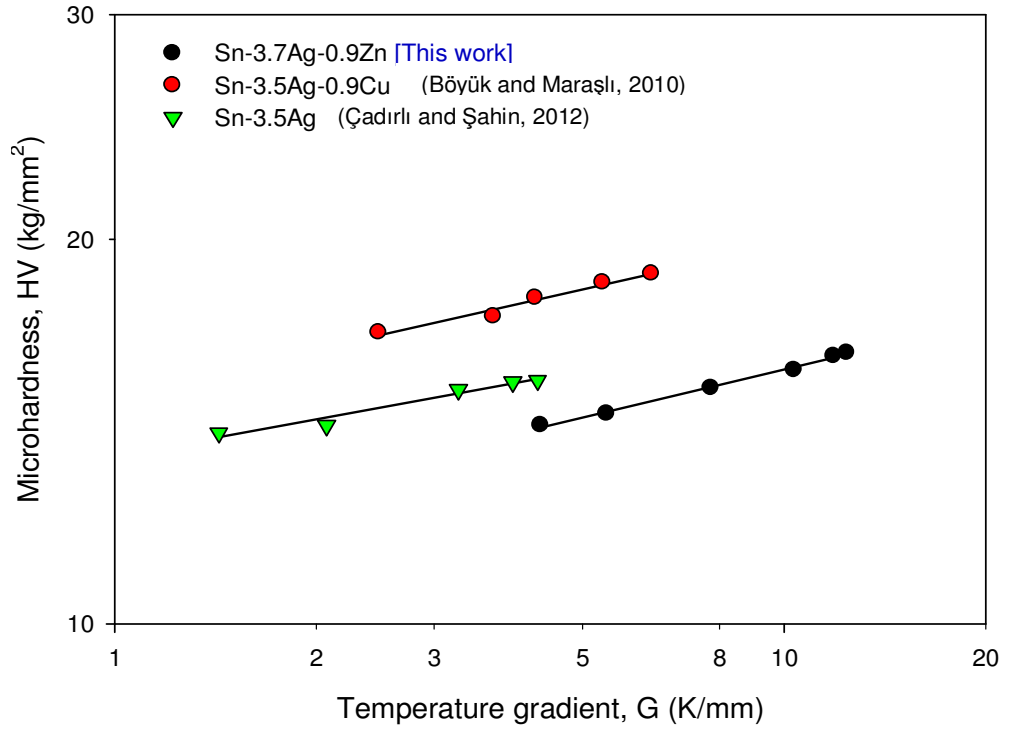

Figure 3. Variation of microhardness, as a function of temperature gradient for directionally solidified Sn-3.7wt.%Ag-0.9wt.%Zn eutectic alloy at a constant growth rate and compare with the Sn-3.5wt.%Ag-0.9wt.%Cu and Sn-3.5wt.%Ag eutectic alloys.

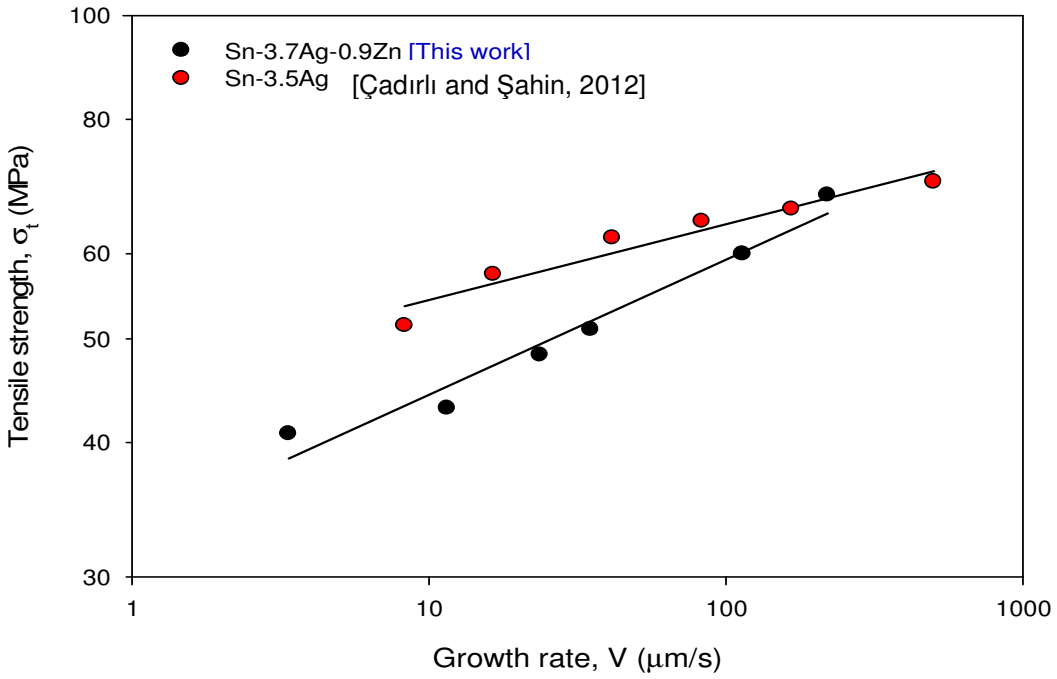

Figure 4. Variation of tensile strength, as a function of growth rate for directionally solidified Sn-3.7wt.%Ag-0.9wt.%Zn eutectic alloy at a constant temperature gradient and compare with the Sn-3.5wt.%Ag eutectic alloys.

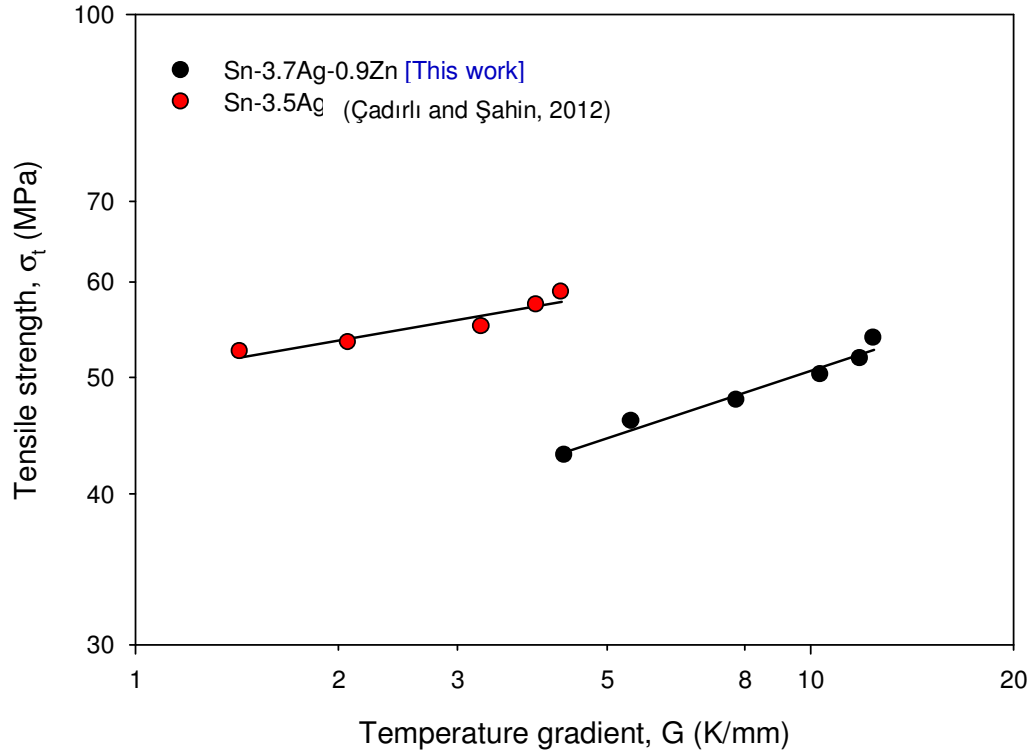

Figure 5. Variation of tensile strength, as a function of temperature gradient for directionally solidified Sn-3.7wt.%Ag-0.9wt.%Zn eutectic alloy at a constant growth rate and compare with the Sn-3.5wt.%Ag eutectic alloys.

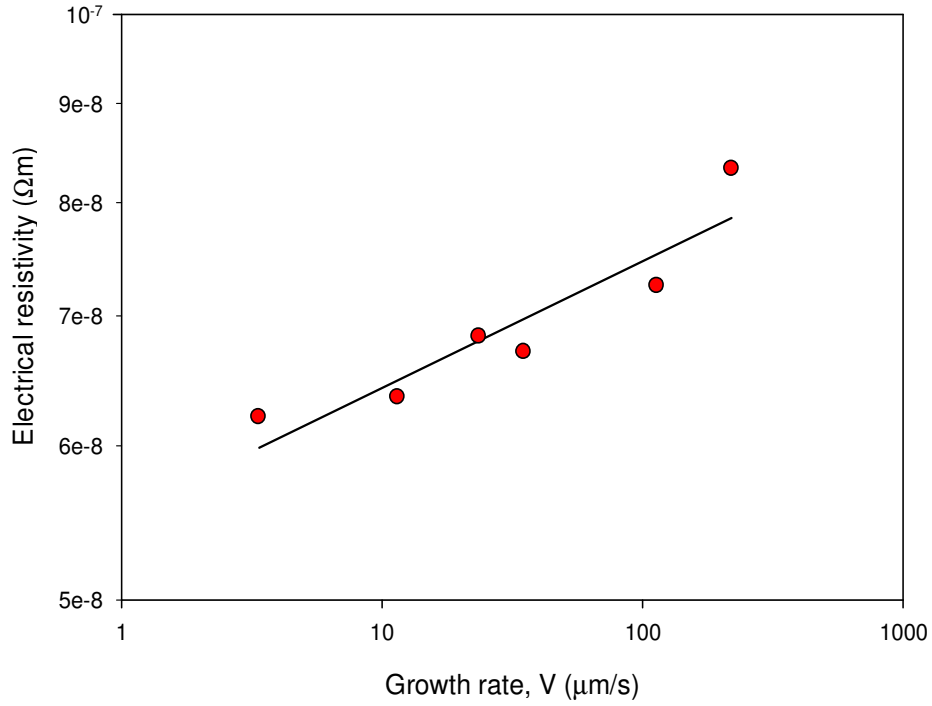

Figure 6. Variation of electrical resistivity, as a function of growth rate for directionally solidified Sn-3.7wt.%Ag-0.9wt.%Zn eutectic alloy at a constant temperature gradient.

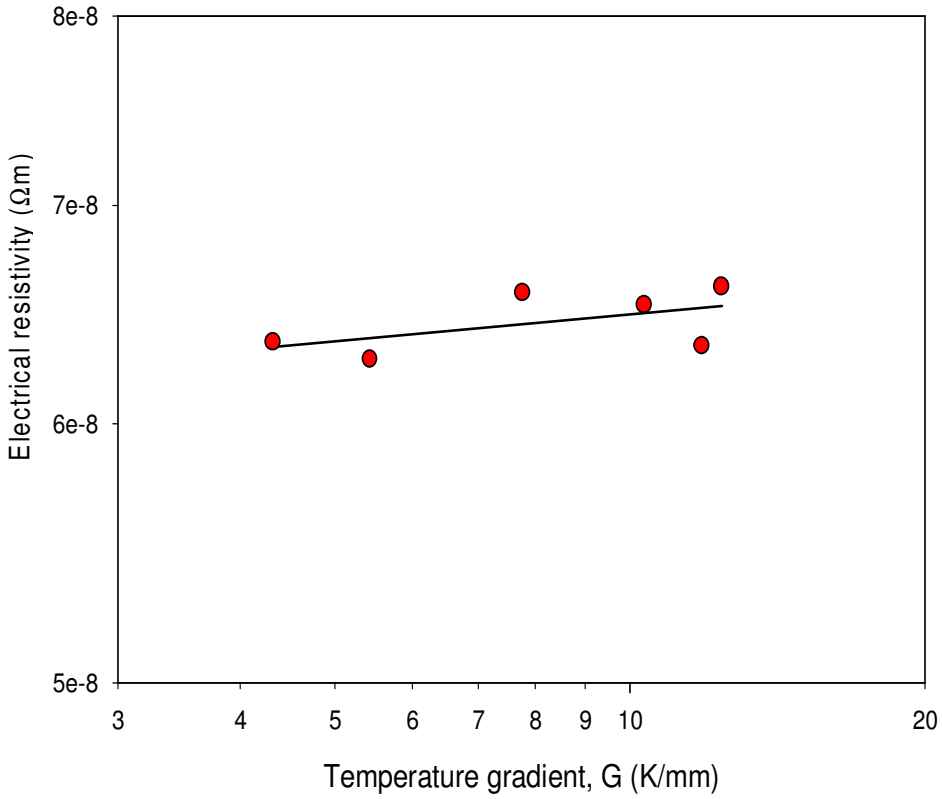

Figure 7. Variation of electrical resistivity, as a function of temperature gradient for directionally solidified Sn-3.7wt.%Ag-0.9wt.%Zn eutectic alloy at a constant growth rate.

Figure 2 shows the variation of HV as a function of V at a constant G. The value of HV increases with the increasing value of V. Using linear regression analysis, the relationship between the HV and V was determined as $HV = 20.65(V)^{0.09}$, and the exponent value was found to be 0.09 for Sn-Ag-Zn eutectic alloy. This exponent value (0.09) agrees with the exponent values of V (0.07–0.11) obtained by various researchers (Böyük and Maraşli, 2009; Vnuk et al., 1979, 1980; Telli and Kisakürek, 1988). for different binary and ternary eutectic alloy systems, under similar solidification conditions.

Using linear regression analysis, the relationship between HV and G was determined as $HV = 11.83(G)^{0.12}$, and the exponent value was found to be 0.12. As can be seen from Figure 3, the value of microhardness increases with the increasing the value of the temperature gradient (G) for a given constant V as well. An exponent value relating to G (0.12) generally agrees with the exponent values relating to obtained in previous experimental works (Böyük and Maraşli, 2010).

Figures 2 and 3 show the maximum and minimum values of HV for Sn-3.7wt.%Ag-0.9wt.%Zn eutectic alloy are lower than the maximum and minimum values of HV obtained by Böyük and Maraşli (2009) and Çadirli and Şahin (2012) for unidirectional solidified Sn-3.5wt.%Ag-0.9wt.%Cu and Sn-3.5wt.%Ag eutectic alloy, respectively. While the microhardness of the Sn-3.5wt.%Ag eutectic alloy decreases with the adding 0.9wt.% of Zn content, conversely increases with the adding 0.9wt.% of Cu. Besides, the microhardness of the slowly cooled Sn-Ag-Zn eutectic solder increased from 14.4 to 17 HV and the rapidly solidified one increased from 15 to 29.1 HV obtained by Wei et al. (2009).

HV values obtained by Wei et al. (2009) for Sn-Ag-Zn eutectic alloy agree with this experimental works for slowly cooled (13.4 to 18.15).

The effect of solidification parameters on tensile strength

Figures 4 and 5 show the variation of the tensile strength values with growth rate and temperature gradient. The dependence of σ_t on the V and G can be represented by equations as follows;

$$\sigma_t = k_3(V)^c \quad (5)$$

$$\sigma_t = k_4(G)^d \quad (6)$$

where k is a constant, c and d are the exponent values relating to the growth rate and temperature gradient, respectively.

From Figure 4, the relationship between σ_t and V was found to be $\sigma_t = 31.62(V)^{0.14}$ by using linear regression analysis and also it can be seen that values of the tensile strength increase with increasing growth rate. It is found that, while growth rate increasing from 3.37 to 220.12 µm/s, the tensile strength increases from 40.75 to 68.00 MPa.

Figure 5 shows the experimental results of tensile strength as a function of the temperature gradient. It can be seen that the value of the tensile strength also increases with increasing temperature gradient. It is 12.41 K/mm, the tensile strength increase from 43.06 to 53.85 MPa. Using linear regression analysis, the relationship between σ_t and G was found to be $\sigma_t = 32.96(G)^{0.19}$.

Figures 4 and 5 show the maximum and minimum values of σ_t for Sn-3.7wt.%Ag-0.9wt.%Zn eutectic alloy are lower than the maximum and minimum values of σ_t obtained by Çadirli and Şahin (2012) for unidirectional solidified Sn-3.5wt.%Ag alloy. Besides, the tensile strength of the Sn–3.5%Ag eutectic alloy decreases with the adding 0.9% of Zn content.

The effect of solidification parameters on electrical resistivity

Figures 6 and 7 show the variation of the electrical resistivity values with growth rate and temperature gradient. The dependence of ρ on the V and G can be represented by equations as follows;

$$\rho = k_5(V)^e \quad (7)$$

$$\rho = k_6(G)^f \quad (8)$$

where k is a constant, e and f are the exponent values relating to the growth rate and temperature gradient, respectively.

From Figures 6 and 7, the relationships between ρ and V, ρ and G were found to be $\rho = 5.62\times10^{-8}(V)^{0.07}$ and $\rho = 6.16\times10^{-8}(G)^{0.04}$ respectively by using linear regression analysis and also it can be seen that values of the electrical resistivity increase with increasing growth rate and temperature gradient (Figures 6 and 7).

Conclusions

In the present work, the influence solidification parameters and temperature on the mechanical, electrical and thermal properties of Sn-3.7wt.%Ag-0.9wt.%Zn eutectic alloy was investigated. The results are summarized as follows;

(1) Values of micro hardness increase with increasing the values of V and G. The establishment of the relationships among HV, V and G can be given as; $HV = 20.65(V)^{0.09}$ and $HV = 11.83(G)^{0.12}$.

(2) The experimental expressions correlating the values of σ_t with the values of V and G for directional solidified Sn-3.7wt.%Ag-0.9wt.%Zn eutectic alloy have shown that the values of the tensile strength increase with increasing the values of V and G. The establishment of the relationships between strength and solidification parameters can be given as; $\sigma_t = 31.62(V)^{0.14}$ and $\sigma_t = 32.96(G)^{0.19}$.

(3) The values of electrical resistivity increase with increasing the values of V and G. The establishment of the relationships among electrical resistivity and solidification parameters can be given as;

$\rho = 5.62 \times 10^{-8}(V)^{0.07}$ and $\rho = 6.16 \times 10^{-8}(G)^{0.04}$.

ACKNOWLEDGEMENTS

This project was supported by Erciyes University Scientific Research Project Unit Contract No: FBT 07–65. The authors are grateful to Erciyes University Scientific Research Project Unit for their financial support.

REFERENCES

Abtew M, Selvaduray G (2000). Lead-free solders in microelectronics. Mater. Sci. Eng. 27:95-141.

Anderson IE, Foley JC, Cook BA, Harringa J, Terpstra RL, Unal O (2001). Alloying effects in near-eutectic Sn-Ag-Cu solder alloys for improved microstructural stability. J. Electron. Mater. 30:1050-1059.

Böyük U, Maraşli N (2009). The microstructure parameters and microhardness of directionally solidified Sn-Ag-Cu eutectic alloy. J. Alloy. Compd. 485:264-269.

Böyük U, Maraşli N (2010). Dependency of eutectic spacings and microhardness on the temperature gradient for directionally solidified Sn-Ag-Cu lead-free solder. Mater. Chem. Phys. 119:442-448.

Böyük U, Maraşli N, Kaya H, Çadirli E, Keşlioğlu K (2009). Directional solidification of Al-Cu-Ag alloy. Appl. Phys. A–Mater. 95:923-932.

Çadirli E, Şahin M (2012). Influence of temperature gradient and growth rate on the mechanical properties of directionally solidified Sn-3.5 wt% Ag eutectic solder. J. Mater. Sci. Mater. Electron. 23:31-40.

Cho MG, Kang SK, Shih DY, Lee HM (2007). Effects of minor additions of Zn on interfacial reactions of Sn-Ag-Cu and Sn-Cu solders with various Cu substrates during thermal aging. J. Electron. Mater. 36: 1501-1509.

Choi WK, Hoi SW, Shih D-Y, Henderson DW, Gosselin T, Sarkhel A, Goldsmith C, Yoon KJ, Lee HM (2001). Effect of in addition on Sn-3.5Ag solder and joint with Cu substrate. Mater. Trans. 42:783-789.

Gündüz M, Kaya H, Çadirli E, Özmen A (2004). Interflake spacings and undercoolings in Al-Si irregular eutectic alloy. Mat. Sci. Eng. A. 369:215-229.

Jeong SW, Kim JH, Lee HM (2004). Effect of cooling rate on growth of the intermetallic compound and fracture mode of near-eutectic Sn-Ag-Cu/Cu pad: Before and after aging. J. Electron. Mater. 33:1530-1544.

Jo YH, Lee JW, Seo S-K, Lee HM, Han H, Lee DC (2008). Demonstration and characterization of Sn-3.0Ag-0.5Cu/Sn-57Bi-1Ag combination solder for 3-D multistack packaging. J. Electron. Mater. 37:110-117.

Kang SK, Cho MG, Shih DY, Seo S-K, and Lee HM (2008). Proc. 58th Electronic Components and Technology Conf. (Piscataway NJ: IEEE. 2008). P. 478.

Kang SK, Choi WK, Shih D-Y, Henderson DW, Gosselin T, Sarkhel A, Goldsmith C, Puttlitz KJ (2003). Ag3Sn plate formation in the solidification of near-ternary eutectic Sn-Ag-Cu. JOM. 55(6):61-65.

Kang SK, Sarkhel AK (1994). Lead (Pb)-Free Solders for Electronic Packaging. J. Electron. Mater. 23:701-707.

Kim DH, Cho MG, Seo S-K, Lee HM (2009). Effects of Co Addition on Bulk Properties of Sn-3.5Ag Solder and Interfacial Reactions with Ni-P UBM. J. Electron. Mater. 38:39-45.

Knott S, Flandorfer H, Mikula A (2005). Calorimetric investigations of the two ternary systems Al-Sn-Zn and Ag-Sn-Zn. Z. Metallkd. 96:38-44.

Liu YC, Wan JB, Gao ZM (2008). Intermediate decomposition of metastable Cu5Zn8 phase in the soldered Sn-Ag-Zn/Cu interface. J. Alloy. Compd. 465:205-209.

Porter DA, Easterling KE (1992). Phase transformations in metals and alloys. Second Edition. CRC Press. P. 185.

Rudnev V, Loveless D, Cook R, Black M (2003). Markel Dekker Inc. New York. P. 119.

Seo SK, Cho MG and Lee HM (2007). Thermodynamic assessment of the Ni-Bi binary system and phase equilibria of the Sn-Bi-Ni ternary system. J. Electron. Mater. 36:1536-1544.

Seo S-K, Cho MG, Choi WK, Lee HM (2006). Comparison of Sn2.8Ag20In and Sn10Bi10In solders for intermediate-step soldering. J. Electron. Mater. 35:1975-1981.

Telli AI, Kisakürek SE (1988). Effect of antimony additions on hardness and tensile properties of directionally solidified Al–Si eutectic alloy. Mat. Sci. Tech. 4:153-156.

Vnuk F, Sahoo M, Baragor D and Smith RW (1980). Mechanical-properties of the Sn-Zn eutectic alloys. J. Mater. Sci. 15:2573-2583.

Vnuk F, Sahoo M, Van De Merwe R, Smith RW (1979). The hardness of Al-Si eutectic alloys. J. Mater. Sci. 14:975-982.

Wang X, Liu YC, Wei C, Gao HX, Jiang P, Yu LM (2009). Strengthening mechanism of SiC-particulate reinforced Sn-3.7Ag-0.9Zn lead-free solder. J. Alloy. Compd. 480:662-665.

Wei C, Liu Y, Gao Z, Xu R, Yang K (2009). Effects of aging on structural evolution of the rapidly solidified Sn-Ag-Zn eutectic solder. J. Alloy. Compd. 468:154-157.

Wei C, Liu YC, Han YJ, Wan JB, Yang K (2008). Microstructures of eutectic Sn-Ag-Zn solder solidified with different cooling rates. J. Alloy. Compd. 464:301-305.

Wu CML, Yu DQ, Law CMT, Wang L (2004). Properties of lead-free solder alloys with rare earth element additions. Mater. Sci. Eng. R. 44:1-44.

Xu RL, Liu YC, Wei C, Yu LM (2010). Effects of Zn additions on the structure of the soldered Sn-3.5Ag and Cu interfaces. Solder. Surf. Mt. Tech. 22(2):13-20.

Zeng K, Tu KN (2002). Six cases of reliability study of Pb-free solder joints in electronic packaging technology. Mater. Sci. Eng. R. 38:55-105.